

Electronic properties of CuO₂-planes: A DMFT study

 M.B. Zöflf^a, Th. Maier, Th. Pruschke, and J. Keller

Institut für Theoretische Physik I, Universität Regensburg, Universitätsstr. 31, 93053 Regensburg, Germany

Received 21 September 1998 and Received in final form 8 June 1999

Abstract. We study one-particle spectra and the electronic band-structure of a CuO₂-plane within the three-band Hubbard model. The Dynamical Mean-Field Theory (DMFT) is used to solve the many particle problem. The calculations show that the optical gap Δ_{opt} is given by excitations from the lower Hubbard band into the so called Zhang-Rice singlet band. The optical gap Δ_{opt} turns out to be considerably smaller than the bare charge transfer energy Δ ($\Delta = \epsilon_p - \epsilon_d$) for a typical set of parameters, which is in agreement with experiment. We also investigate the dependence of the shape of the Fermi surface on the different hopping parameters t_{CuO} and t_{OO} . A value $t_{\text{OO}}/t_{\text{CuO}} > 0$ leads to a Fermi surface surrounding the M point.

PACS. 71.27.+a Strongly correlated electron systems; heavy fermions – 71.30.+h Metal-insulator transitions and other electronic transitions – 74.25.Fy Transport properties (electric and thermal conductivity, thermoelectric effects, etc.)

1 Introduction

Since the discovery of high temperature superconductivity by Bednorz and Müller [1] it is a challenging problem to find a theoretical description of this phenomenon. However, even in the normal state the electronic properties of high- T_c compounds are extremely hard to describe due to electronic correlations. A characteristic feature of the high- T_c compounds is a structure consisting of one or more CuO₂-planes, which are mainly responsible for the electronic properties of these compounds including superconductivity [2].

The most simple theoretical description of such a CuO₂-plane uses the one-band Hubbard model [3], which contains one effective Cu $3d_{x^2-y^2}$ orbital in a tight-binding ansatz. The system becomes nontrivial through the presence of a Coulomb repulsion U_d acting between particles on the same site. This model describes the properties of the so called Mott-Hubbard metal-insulator transition [4] and also contains other important aspects of the physics of the high- T_c compounds like *e.g.* antiferromagnetism. However, the simple one-band Hubbard model leads to a wrong description of the planes concerning the doping dependence of various properties, such as the asymmetric magnetic doping-temperature phase diagram [5].

The oxygen atoms in the CuO₂-plane, respectively the $2p$ -orbitals of these atoms, introduce a further degree of freedom and the strongest hybridization takes place between the Cu- $3d_{x^2-y^2}$ orbital and the O- $2p_{x/y}$ orbitals [6]. Therefore they form the lowest lying bonding state and the

highest lying anti-bonding state. Thus, for a more realistic description of the CuO₂-plane one has to take into account at least these two sets of orbitals, *i.e.* the Cu- $3d_{x^2-y^2}$, which is occupied with one hole in the undoped system, and the O- $2p_{x/y}$ states. The resulting model is known as the three-band Hubbard model or Emery model [7]. As in the standard Hubbard model, one can include all kinds of local two-particle interactions. However for the sake of simplicity all Coulomb energies but the Coulomb energy U_d between two electrons on the same d -orbital are neglected. With this model one is for example able to describe a doped charge transfer insulator, which is an essential aspect of the electronic properties of the CuO₂-planes in a high- T_c compound. Such a three-band model has recently been studied by Schmalian *et al.* [8] using a generalized dynamical mean-field theory (DMFT) and our contribution is based on their approach. Watanabe *et al.* [9] discussed the metal-insulator transition in a two-band Hubbard model in infinite dimensions and discovered the coexistence of metallic and antiferromagnetic phases. This was also found by Maier *et al.* [10], who additionally reported about an asymmetric magnetic doping-temperature phase diagram, which shows, that the antiferromagnetic phase is more stable upon electron doping than upon hole doping.

In this paper the DMFT approach of Schmalian *et al.* [8] for the three-band Hubbard model is used as an approximation for the two-dimensional CuO₂ planes of the high- T_c compounds. At a first glance the use of the DMFT as an approximation to a low-dimensional system may seem to be particularly crude. However, as long as the system is not too close to a phase transition the choice

^a e-mail: markus.zoelfl@rphs1.physik.uni-regensburg.de

of a local selfenergy appears to capture the most important dynamics, which is seen by *e.g.* comparing results from such an approximation to those of a Quantum Monte Carlo calculation for the two-dimensional one-band Hubbard model [11]. In addition to the mere copper-oxygen hopping in the original three-band Hubbard model we also include an oxygen-oxygen hopping process, which is usually considered important especially to determine the correct shape of the Fermi surface.

In Section 2 we first present the model and discuss the DMFT ansatz, which we use for an approximate solution. In Section 3.1 the results for one-particle spectra as function of the oxygen-oxygen hopping amplitude are discussed. As a particularly interesting result we show that the optical gap seen in experiments is set by the separation between the lower Hubbard band and the so-called Zhang-Rice band and is strongly renormalized from its bare value as obtained from the model parameters. In Section 3.2 we investigate in detail the influence of the oxygen-oxygen hopping amplitude parameter on the band-structure and Fermi surface, a summary and outlook in Section 4 concludes the paper.

2 Model Hamiltonian and method

2.1 The three-band Hubbard model

The starting point of our approach is a simplified Emery Hamiltonian [7] describing the dynamics of holes in a doped CuO_2 -plane. The nearest neighbour hopping processes between the $3d$ -orbital of the Cu-atom and the $2p_x$ -/ $2p_y$ -orbital of the O-atom ($t_{i,j\nu}$ and $t'_{i\kappa,j\nu}$) are taken into account. ε_d and ε_p denote the energy levels of each orbital and μ the chemical potential. The local Coulomb energy U_d for the case of a doubly occupied d -orbital is responsible for the correlations.

$$\begin{aligned} \hat{H} = & \sum_{i,\sigma} (\varepsilon_d - \mu) d_{i,\sigma}^\dagger d_{i,\sigma} + \sum_{i,\nu,\sigma} (\varepsilon_p - \mu) p_{i\nu,\sigma}^\dagger p_{i\nu,\sigma} \\ & + \sum_{i,j,\nu,\sigma} (t_{i,j\nu} d_{i,\sigma}^\dagger p_{j\nu,\sigma} + h.c.) \\ & + \sum_{\substack{i,\nu,j,\kappa,\sigma \\ i \neq j, \nu \neq \kappa}} t'_{i\kappa,j\nu} p_{i\kappa,\sigma}^\dagger p_{j\nu,\sigma} + \sum_i U_d d_{i,\uparrow}^\dagger d_{i,\uparrow} d_{i,\downarrow}^\dagger d_{i,\downarrow}. \end{aligned} \quad (1)$$

As mentioned in the introduction, this Hamiltonian is able to describe a doped charge transfer insulator, which is characterized by the charge transfer energy $\Delta = \varepsilon_p - \varepsilon_d$. The relation $U > \Delta$ ensures the system of being in the charge transfer regime [12]. This relation typically holds for parameters obtained from a first principles calculation for the CuO_2 planes under consideration (see Tab. 1). The gauge invariance of the Hamiltonian allows us to choose the phase of the wave functions freely. We use the phase convention shown in Figure 1, which determines all phases of the included hopping processes uniquely. The transformation into \mathbf{k} -space leads us to the following Hamiltonian

Table 1. Parameters for a three-band model (in eV) calculated with a constrained first principles calculation for La_2CuO_4 done by Hybertsen *et al.* [13].

Δ	t	t'	U_d	U_p	U_{pd}	U_{pp}
3.6	1.3	0.65	10.5	4	1.2	0

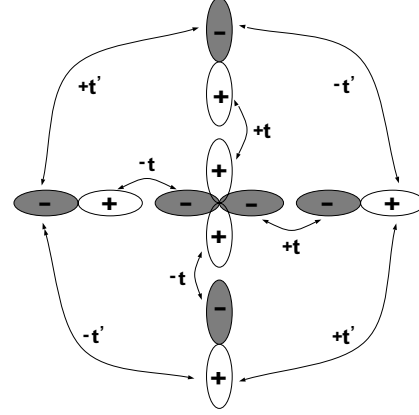


Fig. 1. Used phase convention, which determines the phases of all hopping processes.

(for simplicity we show the non-interacting part only):

$$H_o = \sum_{\mathbf{k},\sigma} (d_{\mathbf{k}\sigma}^\dagger, p_{x\mathbf{k}\sigma}^\dagger, p_{y\mathbf{k}\sigma}^\dagger) \underline{h}(\mathbf{k}) \begin{pmatrix} d_{\mathbf{k}\sigma} \\ p_{x\mathbf{k}\sigma} \\ p_{y\mathbf{k}\sigma} \end{pmatrix}, \quad (2)$$

with the matrix $\underline{h}(\mathbf{k})$:

$$\begin{pmatrix} \varepsilon_d - \mu & 2it \sin(\mathbf{k}\mathbf{r}_x) & 2it \sin(\mathbf{k}\mathbf{r}_y) \\ -2it \sin(\mathbf{k}\mathbf{r}_x) & \varepsilon_p - \mu & -4t' \sin(\mathbf{k}\mathbf{r}_x) \sin(\mathbf{k}\mathbf{r}_y) \\ -2it \sin(\mathbf{k}\mathbf{r}_y) & -4t' \sin(\mathbf{k}\mathbf{r}_x) \sin(\mathbf{k}\mathbf{r}_y) & \varepsilon_p - \mu \end{pmatrix} \quad (3)$$

and the next neighbour distance $\mathbf{r}_x, \mathbf{r}_y$.

2.2 Dynamical mean-field approximation

This uncorrelated part of the Hamiltonian (3) can of course be diagonalized easily. In order to treat the strong Coulomb repulsion U_d , we here introduce the dynamical mean-field theory, *i.e.* we approximate the proper one-particle self energy of the d -states by a purely local quantity, $\Sigma(\mathbf{k}, z) \rightarrow \Sigma(z)$. This allows to map the lattice problem onto an effective Anderson impurity model [14] hybridizing with fictitious conduction electrons (holes in our case). The locality of the self-energy and the resulting mapping onto an effective impurity model becomes exact in the limit of infinite coordination number [16] and has been extensively and successfully used to study the properties of the one-band Hubbard model [17]. As has been pointed out by Gross and Valenti [15] the model (1) can in principle be generalized to D dimensions, too, but in

contrast to the Hubbard model it is impossible to find a uniform scaling to obtain a nontrivial limit $D \rightarrow \infty$. The DMFT therefore always leads to an approximate treatment for the three band Hubbard model.

As first step of our derivation of the cluster/impurity we apply a unitary transformation to the Hamiltonian (2):

$$H = \sum_{\mathbf{k}, \sigma} (d_{\mathbf{k}\sigma}^\dagger, p_{\mathbf{k}\sigma}^\dagger, \bar{p}_{\mathbf{k}\sigma}^\dagger) \begin{pmatrix} \varepsilon_d - \mu & -2t\gamma_{\mathbf{k}} & 0 \\ -2t\gamma_{\mathbf{k}} & \varepsilon_{p\mathbf{k}} - \mu & t'_{\mathbf{k}} \\ 0 & t'_{\mathbf{k}} & \varepsilon_{\bar{p}\mathbf{k}} - \mu \end{pmatrix} \begin{pmatrix} d_{\mathbf{k}\sigma} \\ p_{\mathbf{k}\sigma} \\ \bar{p}_{\mathbf{k}\sigma} \end{pmatrix} \quad (4)$$

with

$$\varepsilon_{p\mathbf{k}} = \varepsilon_p - \frac{8t'}{\gamma_{\mathbf{k}}^2} \sin(\mathbf{k}x)^2 \sin(\mathbf{k}y)^2, \quad (5)$$

$$\varepsilon_{\bar{p}\mathbf{k}} = \varepsilon_p + \frac{8t'}{\gamma_{\mathbf{k}}^2} \sin(\mathbf{k}x)^2 \sin(\mathbf{k}y)^2, \quad (6)$$

$$t'_{\mathbf{k}} = \frac{4t' \sin(\mathbf{k}x) \sin(\mathbf{k}y)}{\gamma_{\mathbf{k}}^2} \{\sin(\mathbf{k}x)^2 - \sin(\mathbf{k}y)^2\} \quad (7)$$

and

$$\gamma_{\mathbf{k}}^2 = \sin(\mathbf{k}x)^2 + \sin(\mathbf{k}y)^2. \quad (8)$$

This transformation introduces new orbitals p and \bar{p} . d hybridizes with p but not with \bar{p} . The case of $t' = 0$ leads to a dispersionless \bar{p} -band at $\varepsilon_p - \mu$ and the \bar{p} -orbital is decoupled from the rest of the system. This procedure leads to a well-defined description of local orbitals at different lattice cells, which was already suggested by Valenti and Gros [15], and solves the problem how to distribute the p -orbitals, which originally are located in between different Cu-sites to a particular unit cell. In order to construct a sensible DMFT we here follow a path, which identifies the effective 'impurity' needed to set up the DMFT equations directly from the local d Green's function. Due to the form (4) of the Hamiltonian the general structure for $G_{\mathbf{k}\sigma}^{dd}(z)$ within the DMFT is:

$$G_{\mathbf{k}\sigma}^{dd}(z) = \left[z - \varepsilon_d + \mu - \Sigma_d(z) - \frac{4t^2\gamma_{\mathbf{k}}^2}{z - \varepsilon_{p\mathbf{k}} + \mu - \frac{t_{\mathbf{k}}^2}{z - \varepsilon_{\bar{p}\mathbf{k}} + \mu}} \right]^{-1}. \quad (9)$$

The sum over \mathbf{k} , which is needed to calculate the local Green's function, will in general lead to a complicated structure in the denominator. However, since the self energy $\Sigma_d(z)$ is \mathbf{k} -independent we may cast it into the form:

$$G_{\mathbf{k}\sigma}^{dd}(z) = \frac{1}{N} \sum_{\mathbf{k}} G_{\mathbf{k}\sigma}^{dd}(z) \stackrel{!}{=} \left[z - \varepsilon_d + \mu - \Sigma_d(z) - \frac{t^2}{z - \hat{\varepsilon}_p + \mu - \Delta(z)} \right]^{-1}, \quad (10)$$

where \hat{t} and $\hat{\varepsilon}_p$ are defined through

$$\begin{aligned} \hat{t} &= -2t \sum_{\mathbf{k}} \gamma_{\mathbf{k}} \\ \hat{\varepsilon}_p &= \sum_{\mathbf{k}} \varepsilon_{p\mathbf{k}} \end{aligned} \quad (11)$$

respectively. The effective hybridization function $\Delta(z)$ is defined through equation (10) and incorporates all band-structure effects due to the dispersion and hybridizations. Note that this definition is far from being unique! In fact we may choose for example

$$\frac{1}{N} \sum_{\mathbf{k}} G_{\mathbf{k}\sigma}^{dd}(z) \stackrel{!}{=} [z - \varepsilon_d + \mu - \Sigma_d(z) - \tilde{\Delta}(z)]^{-1} \quad (12)$$

as another possibility. In this case the equation defining the DMFT would be formally the same as for the one-band Hubbard model [17]. However, due to the singular structure introduced by the d - p -hopping, equation (10) turns out to be numerically more convenient: For $\Delta(z) = 0$ the level structure of the d - p complex is already included from the outset and the final $\Delta(z)$ is rather smooth. On the other hand, the at a first glance more natural choice (12) would result in a $\tilde{\Delta}(z)$ with a highly singular behaviour close to ε_p reflecting the existence of unrenormalized p -states. Thus the Hamiltonian of the effective impurity is defined as:

$$\begin{aligned} H &= \sum_{\sigma} (\varepsilon_d - \mu) d_{\sigma}^{\dagger} d_{\sigma} + \sum_{\sigma} (\hat{\varepsilon}_p - \mu) p_{\sigma}^{\dagger} p_{\sigma} \\ &+ \sum_{\sigma} (\hat{t} d_{\sigma}^{\dagger} p_{\sigma} + h.c.) + U_d d_{\uparrow}^{\dagger} d_{\downarrow} d_{\uparrow}^{\dagger} d_{\downarrow} \\ &+ \sum_{\mathbf{k}, \sigma} (V_{\mathbf{k}} p_{\sigma}^{\dagger} c_{\mathbf{k}, \sigma} + h.c.) + \sum_{\mathbf{k}, \sigma} \varepsilon_{\mathbf{k}} c_{\mathbf{k}, \sigma}^{\dagger} c_{\mathbf{k}, \sigma}, \end{aligned} \quad (13)$$

with a hybridization $V_{\mathbf{k}}$ of the p -orbitals to the effective medium described by the dispersion $\varepsilon_{\mathbf{k}}$. The effective medium enters the solution of the impurity problem only *via* the hybridization function

$$\Delta(z) = \frac{1}{N} \sum_{\mathbf{k}} \frac{|V_{\mathbf{k}}|^2}{z - \varepsilon_{\mathbf{k}}}. \quad (14)$$

of the p -states and has to be determined selfconsistently from equation (10).

Equation (10) is the central point of our selfconsistency scheme. After calculating the local Green's function *via* the \mathbf{k} -sum of equation (9) one can extract the hybridization function $\Delta(z)$, which is used to solve the impurity problem. This non-trivial step is currently done with the help of an extended NCA scheme [8]. From the impurity Green's function for the d -orbital we extract the selfenergy $\Sigma(z)$, which is then used in the calculation of the lattice Green's function in equation (10).

3 One-particle properties and optical spectra

In this section we present results for the single-particle spectra of the model (1) on a two-dimensional square lattice. Since the complicated structure of the dispersions in

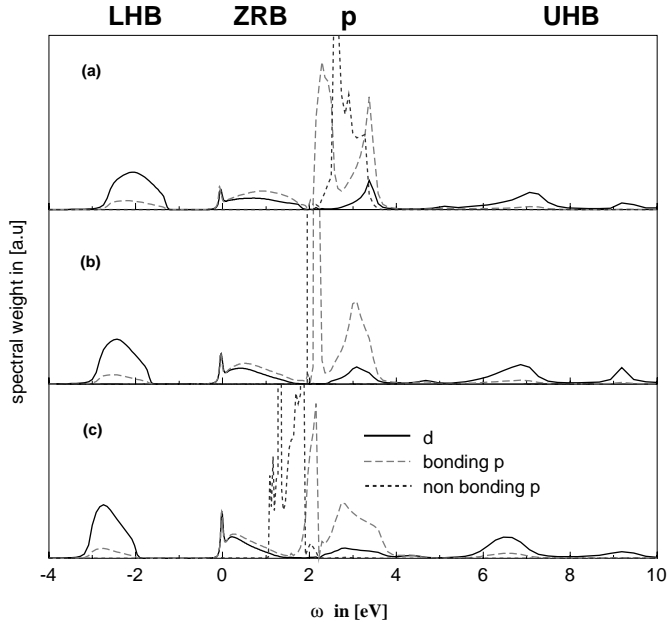


Fig. 2. One-particle spectra of the d - (full curve), the binding p - (dashed curve) and the non-binding p -orbital (dotted curve) for +5% hole doping with $t' = 0.2$ (a), $t' = 0$ (b) and $t' = -0.2$ (c). The other parameters are: $\beta = 40.0 \text{ eV}^{-1}$, $\Delta = 3.6 \text{ eV}$, $t = 1.0 \text{ eV}$ and $U_d = 7.2 \text{ eV}$. The abbreviations are: LHB = lower Hubbard band, ZRB = Zhang-Rice band, p = p -band and UHB = upper Hubbard band.

(5-7) prohibits an analytic transformation of the \mathbf{k} -sums into spectral integrals we use standard Brillouin zone integration techniques to calculate the local d -Green function (10).

3.1 Local density of states

Let us begin the discussion of the single particle properties of the three-band Hubbard model by considering the standard case $t' = 0$ first. The non-hybridizing \bar{p} -orbital then decouples from the rest of the system leading to a two-band problem. Figure 2b shows a hole doped system with $x = 5\%$ at room temperature, *i.e.* at a reciprocal temperature of $\beta = 40 \text{ eV}^{-1}$. The model parameters are taken from Table 1. The spectra show several characteristic features, namely in terms of the hole picture from the left to the right: the lower Hubbard band, the Zhang-Rice band mostly due to excitations into a d - p singlet state, the p -band and the upper Hubbard band, which has a double peak structure due to the complex excitation capabilities of the cluster under consideration. In addition to those expected structures a sharp resonance appears near the Fermi energy. From the DMFT of the one-band Hubbard model it is well known [17], that this resonance is connected to a local Kondo-like screening. It thus is frequently termed Abrikosov-Suhl resonance to stress the similarity of its physics to the Kondo effect.

One interesting observation can already be made from these spectra. The optical gap Δ_{opt} , which is given by

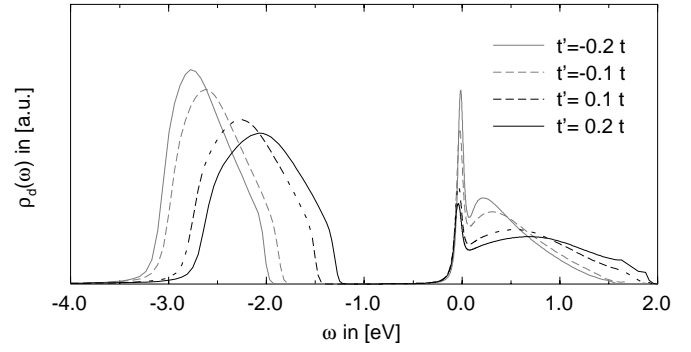


Fig. 3. One-particle spectra of the d orbital near the Fermi energy for different values of t'/t for the same set of parameters as in Figure 2.

the energy separation of the lower Hubbard band and the Zhang-Rice band, is smaller than the bare charge transfer energy $\Delta = \varepsilon_p - \varepsilon_d$. For the present set of parameters we find for example $\Delta_{\text{opt}} \approx 2 \text{ eV}$, which is in agreement with measurements by Uchida *et al.* [18] for $\text{La}_{2-x}\text{Sr}_x\text{CuO}_4$ and $\text{Nd}_{2-x}\text{Ce}_x\text{CuO}_{4-y}$. An optical gap estimated by the bare charge transfer energy $\Delta = 3.6 \text{ eV}$, which is the separation of the lower Hubbard band and the p band, would on the other hand be far too large.

Let us now turn to the effect of a finite t' on the one-particle DOS. Figure 2 summarizes the variation of the DOS of the d -states (full line), the binding p -states (dashed curve) and the non-binding p -states (dotted curve) as function of t' for $t' = -0.2, 0.0, 0.2$ and a hole doping $\delta = 5\%$. As is to be expected, the most drastic effects occur in the DOS of the p -states that shows characteristic fine structures in the vicinity of ε_p connected to the presence of dispersing \bar{p} -states for $t' \neq 0$. The d -states seem at a first glance rather insensitive to t' . However, a closer inspection of the region around the Fermi energy in Figure 3 reveals that with increasing values of t' a reduction of the optical gap occurs. At the same time the energy scale connected to the ASR in the Zhang-Rice band is also decreased, *i.e.* correlation effects appear to be enhanced. The observed reduction of Δ_{opt} can be readily understood by inspecting the behaviour of the level structure of the fundamental copper-oxide cluster. Within the hole picture, the lowest lying states are the singly occupied d -state (filled with one hole) and the d - p -singlet state, which becomes the Zhang-Rice band in the lattice. The energies of these states are given by ε_d and ε_{pd} , which is determined by diagonalization of the cluster. By increasing t' one reduces the energy of the binding p -orbital, and thus $\varepsilon_d - \varepsilon_{pd}$ decreases, *i.e.* the gap in the continuous spectra of the lattice becomes smaller.

The increasing influence of correlations on the other hand can be accounted for by the fact, that the center of mass of the Zhang-Rice band ε_{ZRB} slowly shifts away from the Fermi level as t' increases. Since the energy scale T^* associated with the quasi-particle peak should roughly scale like $\ln T^* \sim -|\varepsilon_{\text{ZRB}}|$, we obtain the observed decrease of T^* as t' increases. Note that due to the exponential

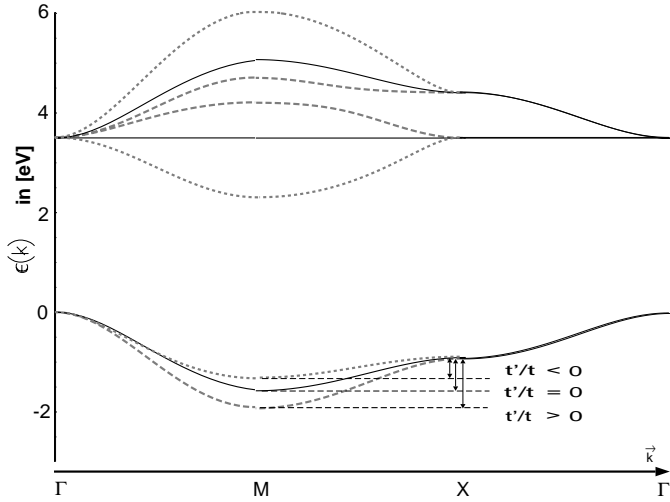


Fig. 4. Tight-binding bandstructure for several values of t'/t . $\varepsilon_d = 0$ eV, $\varepsilon_p = 3.6$ eV, $t = 1$ eV and $t' = 0, \pm 0.3$ eV.

scaling a small shift in ε_{ZRB} will in general strongly change T^* .

3.2 Bandstructure and Fermi surface

Before we discuss the \mathbf{k} -resolved spectral properties of the three-band Hubbard model, let us first look at the uncorrelated tight-binding bandstructure, which is shown in Figure 4. In the following we name the different bands according to their main orbital character. The band with the lowest energy (hole picture) has primarily d -character, while the upper bands have p -character. For hole-doping the Fermi energy lies in the upper bands, for electron-doping in the lower band, consistent with the experimental observations for the CuO_2 planes. The d -band has a minimum at the M-point and a saddle point at the X-point and with increasing value of t'/t the distance between the minimum and the saddle point increases. For comparison with experiment this means that for electron doping the Fermi surface would always surround the M-point for $t' \geq 0$ but would eventually shift to the X-point for $t' < 0$.

In the hole doped case, however, it is evident from Figure 4 that a value of $t'/t \geq 0$ always leads to a Fermi surface centered around Γ . On the other hand, a value $t'/t < 0$ pushes down the non-hybridizing \bar{p} -band, leading to a dispersion minimum at the M-point, as it is observed experimentally [19]. Thus the requirement of a Fermi surface surrounding the M-point for both electron and hole doping means that one either has to assume different signs for t' in the two cases of doping or look for a more subtle mechanism leading to the observed physics for a fixed sign of t' .

In the following we want to argue that in order to solve the puzzle of the correct choice of the parameter t' , one has to consider electronic correlations. In order to make contact with the free bandstructure we plot the spectral function $A(\mathbf{k}, \omega)$ in a density-plot in the ω - \mathbf{k} -plane. The dark regions refer to high spectral weight. In

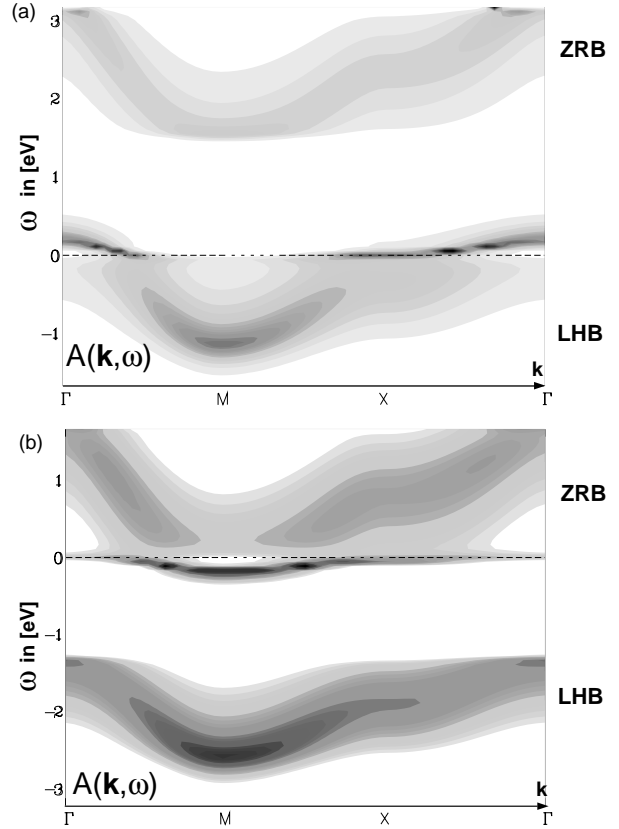


Fig. 5. Spectral function $A(\mathbf{k}, \omega)$ in a density-plot in the ω - \mathbf{k} -plane for special \mathbf{k} -points for $\beta = 40$ eV $^{-1}$, $t = 1$ eV, $t' = 0.3$ eV, $\Delta = 3.6$ eV, $U_d = 7.2$ eV and $x = -8.5\%$ (a), $x = +8.5\%$ (b).

Figures 5a and 5b the low energy part of the resulting \mathbf{k} -dependent total spectral weight for the electron and hole doped CuO_2 -plane is shown. These plots show the lower Hubbard band, the Abrikosov-Suhl resonance and the Zhang-Rice band. These bands all exhibit the typical dispersion of the tight-binding d -band. On the other hand the p -bands and the upper Hubbard band at higher energies (not shown in the figure) have the dispersion of their uncorrelated counterparts. For both types of doping there occurs a quasi-particle resonance at the Fermi energy. It is important to note, that the dispersion of this band (which has mainly d -character) completely determines the shape of the Fermi surface. From the discussion of Figure 3 it became already evident, that a change in t' could change the behaviour of the spectrum close to μ drastically. It is therefore interesting to study the behaviour of $A(\mathbf{k}, 0)$ and thus the variation of the Fermi surface as function of t' more closely. To this end, we plot $A(\mathbf{k}, 0)$ as function of \mathbf{k} in the irreducible part of the first Brillouin zone in Figure 6 as a density plot. The quasi-particle peak manifests itself as a dark region (high intensity). In order to show more closely the shape of the Fermi surface we included lines of constant density in Figure 6, too. From this figure it is apparent, that for constant doping parameter $x = +5\%$, one can change the shape of the Fermi surface by varying

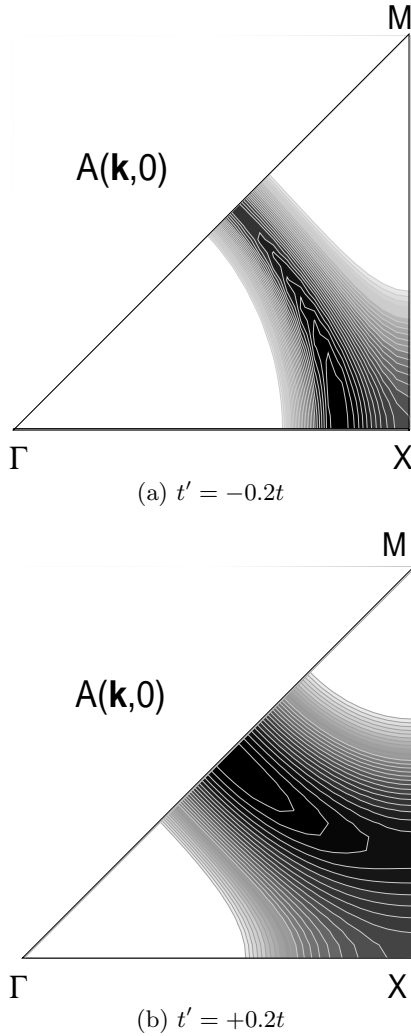


Fig. 6. Total spectral weight at the Fermi energy in a density-plot for two values of t'/t in the irreducible part of the Brillouin zone. The doping is $x = +5\%$ in both cases, the remaining parameters are the same as in Figure 5. One can see that the choice of t'/t determines the shape of the Fermi surface.

the value of t'/t from being electron like ($t' < 0$) with its center at the Γ -point to being hole like ($t' > 0$), *i.e.* surrounding M. In the case of electron doping the sign of t' is of no importance. The Fermi surface always surrounds M here. From the experimental fact that the Fermi surface always encloses the M-point we are led to a value $t'/t > 0$, which is in agreement with results for high- T_c compounds such as $\text{Nd}_{2-x}\text{CeCuO}_4$ [20] or $\text{Bi}_2\text{Sr}_2\text{CaCu}_2\text{O}_{8+x}$ [21].

4 Summary

In this paper we presented results for the optical properties of the two dimensional CuO_2 -plane modeled by the three-band Hubbard Hamiltonian. In order to obtain a more realistic tight-binding bandstructure, direct oxygen-oxygen-hopping processes are also included in addition

to the standard copper-oxygen hybridization. The model was solved with the Dynamical Mean-Field approximation based on previous work by Schmalian *et al.* [8]. The use of this approximation to a 2D system seems justified since we are interested in the electronic properties at finite doping and room temperature, where correlations due to antiferromagnetic and superconducting fluctuations play a minor role. Under these conditions the DMFA was previously shown to be a quite reliable approximation. For the actual calculations we used the actual 2D perovskite type lattice and performed all \mathbf{k} sums using standard Brillouin zone integration techniques. The parameters for the model were taken from the work of Hybertsen *et al.* [13].

The spectra show the well-known structures, namely lower Hubbard band and Zhang-Rice band close to the Fermi energy, and the p - and upper Hubbard bands at higher energies. In addition a quasi-particle peak due to many-body renormalizations appears at the Fermi energy, which is located at the bottom of the Zhang-Rice band for hole and at the top of the lower Hubbard band for electron doping. This quasi-particle band appears to be especially important for the shape of the Fermi surface of the system.

An important result for a comparison to experiment is the optical gap, *i.e.* the difference between bottom of the Zhang-Rice band and top of the lower Hubbard band, is considerably smaller and of the order of experimental values compared to the bare charge transfer gap of the Hubbard model. This value of the gap is further reduced by increasing the oxygen-oxygen hopping-integral. The energy scale connected with the quasi-particle peak at the Fermi energy is also reduced strongly with increasing t'/t . Since this dynamic many-body resonance gives rise to anomalous transport properties at temperatures on the order of the corresponding low-energy scale [17], the inclusion of t' appears to be particularly important to guarantee optical anomalies for energies of the order eV together with transport anomalies for energies of the order 10^{-2} eV.

Further support for the importance of the interplay of correlations and bandstructure effects was obtained from studying the Fermi surface of the system. Experimentally, one expects a Fermi surface centered around the M point of the Brillouin zone for both hole and electron doping. Without correlations however, this could not be guaranteed by a unique choice of the sign of t' , while the inclusion of correlations predicts a unique, and experimentally confirmed, sign, namely $t' > 0$.

One other interesting aspect not mentioned in in this work is the possibility to lift the degeneracy of the oxygen p -states, *i.e.* introduce $\varepsilon_p \rightarrow \{\varepsilon_{p_x}, \varepsilon_{p_y}\}$ and to treat static lattice distortions *via* a value $\varepsilon_{p_x} - \varepsilon_{p_y} \neq 0$. This can be used to study electron-phonon coupling and related effects, which may be important to understand the superconductivity in these materials. Work along this is in progress.

This work was partially supported by the DFG grant PR 298/5-1.

References

1. J.G. Bednorz, K.A. Müller, *Z. Phys. B* **64**, 189 (1986).
2. E. Dagotto, *Rev. Mod. Phys.* **66**, 763 (1994).
3. J. Hubbard, *Proc. Roy. Soc. A* **276**, 238 (1963); J. Kanamori, *Prog. Theor. Phys.* **30**, 275 (1963); M.C. Gutzwiller, *Phys. Rev. Lett.* **10**, 59 (1963).
4. N.F. Mott, *Metal-Insulator Transitions*, 2nd edn. (Taylor and Francis, London, 1990).
5. C. Almasan, M.B. Maple, *Chemistry of High-Temperature Superconductors*, edited by C.M. Rao (World Scientific, Singapore, 1991).
6. P. Fulde, *Electron Correlation in Molecules and Solids* (Springer-Verlag, Berlin Heidelberg, 1995) 14.2.
7. V. Emery, *Phys. Rev. Lett.* **58**, 2794 (1987).
8. J. Schmalian, P. Lombardo, M. Avignon, K.H. Benneman, *Physica B* **223-224**, 602 (1996); P. Lombardo, M. Avignon, J. Schmalian, K.H. Benneman, *Phys. Rev. B* **54**, 5317 (1996).
9. H. Watanabe, S. Doniach, *Phys. Rev. B* **57**, 3829 (1998).
10. Th. Maier, M. Zöfl, Th. Pruschke, J. Keller, *Eur. Phys. J. B* **7**, 377 (1999).
11. Th. Pruschke, Th. Obermeier, J. Keller, M. Jarrell, *Physica B* **223, 224**, 611 (1996).
12. J. Zaanen, G.A. Sawatzky, J.W. Allen, *Phys. Rev. Lett.* **55**, 418 (1985).
13. M.S. Hybertsen, E.B. Stechel, M. Schlüter, D.R. Jennison, *Phys. Rev. B* **41**, 11068 (1990).
14. P.W. Anderson, *Phys. Rev.* **124**, 41 (1961).
15. R. Valenti, C. Gros, *Z. Phys. B* **90**, 161 (1993).
16. W. Metzner, D. Vollhardt, *Phys. Rev. Lett.* **62**, 324 (1989).
17. Th. Pruschke, *Adv. Phys.* **44**, 187 (1995); A. Georges, G. Kotliar, W. Krauth, M.J. Rozenberg, *Rev. Mod. Phys.* **68**, 13 (1996).
18. S. Uchida, T. Ido, H. Takagi, T. Arima, Y. Tokura, S. Tajima, *Phys. Rev. B* **43**, 7942 (1991).
19. Z.X. Shen, D.S. Dessau, *Phys. Rep.* **253**, 1-162 (1995).
20. D.M. King, Z.-X. Shen, D.S. Dessau, B.O. Wells, W.E. Spicer, A.J. Arko, D.S. Marshall, J. DiCarlo, A.G. Loeser, C.H. Park, E.R. Ratner, J.L. Peng, Z.Y. Li, R.L. Greene, *Phys. Rev. Lett.* **70**, 3159 (1993).
21. D.S. Dessau, Z.-X. Shen, D.M. King, D.S. Marshall, L.W. Lombardo, P.H. Dickinson, A.G. Loeser, J. DiCarlo, C.H. Park, A. Kapitulnik, W.E. Spicer, *Phys. Rev. Lett.* **71**, 2781 (1993).